

# Characterization methods of low frequency RTS noise in cooled infrared detectors

Maxence GUENIN  
*Département Optique et Techniques  
 Associées  
 ONERA*  
 Palaiseau, FRANCE  
 maxence.guenin@onera.fr

Sophie DERELLE  
*Département Optique et Techniques  
 Associées  
 ONERA*  
 Palaiseau, FRANCE  
 sophie.derelle@onera.fr

Marcel CAËS  
*Département Optique et Techniques  
 Associées  
 ONERA*  
 Palaiseau, FRANCE  
 marcel.caes@onera.fr

Laurent RUBALDO  
*Development & Production  
 Sofradir*  
 Veurey-Voroize, France  
 laurent.rubaldo@sofradir.com

Isabelle RIBET-MOHAMED  
*Département Optique et Techniques  
 Associées  
 ONERA*  
 Palaiseau, FRANCE  
 isabelle.ribet@onera.fr

**Abstract**— Two methods of detection and characterization of blinking pixels are presented and compared. The first one is based on the time-scaled signal and the other is based on the power spectral density of the signal. These methods are then applied on a temperature dependent measurement. It is then shown that the number of RTS pixels and the blinking frequency follow a Boltzmann behavior.

**Keywords**— *Focal Plane Arrays, Infrared, Random Telegraph Signal, Low Frequency Noise, Spectroscopy*

## I. INTRODUCTION

Within the frame of High Operating Temperature (HOT) infrared focal plane arrays (FPAs), low frequency noise, otherwise called  $1/f^\alpha$  noise [1], is one of the main issues to tackle in terms of long term stability of the image quality. It contributes to the degradation of the images quality. And then it decreases the time before a two-point correction is needed. Studies are led to uncover the predominant low frequency contributor to the degradation of RFPN in visible CMOS [2] and infrared FPAs [3][4][5][6]. Therefore, obtaining a physical understanding of the main sources of  $1/f^\alpha$  noise, such as Random Telegraph Signal (RTS), is critical to improve the detectors image stability.

A RTS pixel, usually called “blinking pixel” has its temporal signal fluctuating between two or multiple stable states. It is characterized by the amplitude jump between these states, and the mean state lifetime. If we define the states as:  $\{1\}, \{2\}, \dots, \{N\}$ , the blinking frequency is defined as follows:

$$f_c = \sum_{i=1}^N \frac{1}{\langle \tau_i \rangle} \quad (1)$$

with  $\langle \tau_i \rangle$  the mean lifetime of the level  $i$ . Fig.1 shows an example of a bi-stable RTS pixel, with its associated amplitude and mean lifetimes. Since the lifetime distribution for one single pixel is random, we can also assign it a Gaussian distribution with a standard deviation  $\sigma_\tau$ . The amplitudes and lifetimes greatly differ from one blinking pixel to another, which makes them difficult to detect systematically.

In the first part of this paper, our RTS pixels detections and characterization methods and algorithms are described. The first method is based on Pruned Exact Linear Time (PELT) algorithm [7]. It is used to detect and characterize blinking pixels. The second method is Low Frequency

Noise Spectroscopy (LFNS) [4], which is, in our case, solely used for characterization. In a second part, preliminary Arrhenius plot results obtained with both methods are presented and discussed.

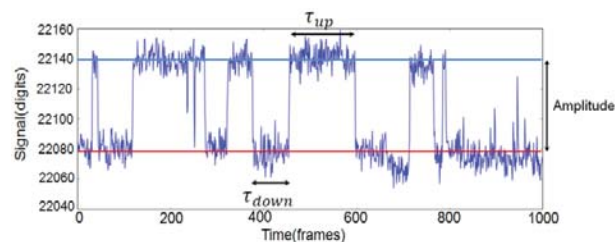


Fig. 1. Typical bi-stable RTS signal over time and its different properties..

## II. RTS PIXELS DETECTION AND CHARACTERIZATION

RTS pixels detection and preliminary characterization in HgCdTe FPAs have already been achieved in the case of bi-stable signals in [8]. RTS pixels with random white noise will present multiple Gaussians on their temporal signal histogram. These Gaussians can then be fitted and if there is more than one, we may assume the pixel has RTS noise. Their mean value gives us information about the amplitude of the telegraph signal. Multiple Gaussians fitting method may be used in the case of multi-stable RTS pixels. However, the characterization based on this method, developed by *Yuzhelevski et al.* [9] is not trivial in the case of multi-stable pixels, and at the moment we are only able to extract RTS lifetime parameters for bi-stable pixels with this technique.

Thus, we used an optimized changepoint detection algorithm presented in [7], which is called “Pruned Exact Linear Time” (PELT) method. Given a set of data  $X$ , we can define a cost function well-suited to a normal distribution with changing mean, and a variance criterion as follows:

$$Cr = \max(k \cdot MAD(X), \frac{\max(X) - \min(X)}{2k})$$

where  $MAD$  is the Median Absolute Deviation of the data, and  $k$  a sensibility factor.

This criterion is mostly empirical but derives from the idea of locating the segments of data which are the furthest from the Gaussian behavior. Using the PELT algorithm, the local minima of the cost function are found, then providing the position of the data changepoints. At this point of the algorithm, there are as many “states” as there are changepoints. In order to access the real values of the states,

we attribute each point of the signal to one of the states with a “State Reduction” (SR) algorithm we developed. It uses the following criterion on the pixel’s non-RTS Gaussian noise: if the difference between two states is lower than  $m$  times the white noise of the signal, these two levels are equivalent to a state with a level equal to their mean value. The coefficient  $m$  is empirical, and may be adjusted. However it is most of the time close to 2. The lifetime distribution of each state can then be obtained, with its mean value and standard deviation. Fig. 2a) and b) shows PELT changepoint fit in two types of cases: high jump amplitude-to-noise ratio and low jump amplitude-to-noise ratio. We can see that in both cases, the PELT curves (in red) match well the bi-stable and multi-stable telegraph signal (in blue). Fig. 2c) shows 2b) associated histogram, and highlights the difficulty to fit Gaussians on this histogram.

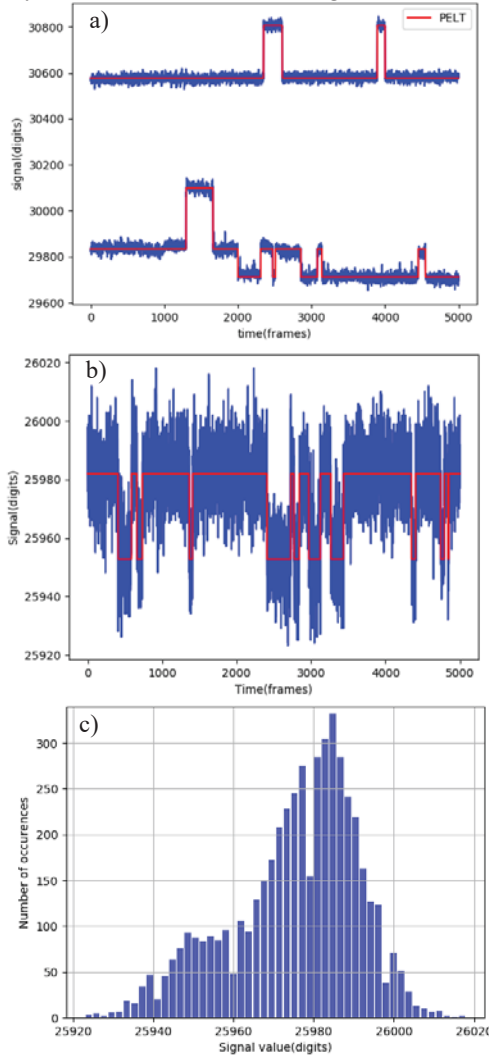


Fig. 2. RTS detected pixel signals (blue curve) and the visualization of their PELT-estimated bi-stable and multi-stable states (red curve) in different cases: a) high jump amplitude-to-noise ratio case, b) low jump amplitude-to-noise ratio case, with c) its associated histogram.

This PELT method is independent from state lifetimes, which gives as much weight to short-lived states as to long-lived states and enables the detection of RTS pixels with unbalanced lifetimes (for example:  $\tau_{down} > \tau_{up}$ ). But it also

makes the spike-typed signals (very short and random pulses) more detectable and therefore brings false alarms. The other main associated drawback is its slightly higher tendency to detect changepoints along low frequency drift. This effect is mainly corrected by our SR algorithm but errors, such as detecting very slow drift noise as RTS, can still be noted, as the confirmation of the algorithm remains visual.

In order to confirm the veracity of the mean lifetime values extracted with PELT method, Low Frequency Noise Spectroscopy (LFNS) [10][11][12] is systematically applied on samples with a sufficient amount of images (min. 5k images, typ. 50k images). The LFNS spectrum is the Power Spectral Density (PSD) spectrum multiplied by the frequency. As mentioned in the introduction, RTS noise is part of the “ $1/f^\alpha$ ” low frequency sources of noise of the spectrum, where  $\alpha$  mainly ranges between 1.0 and 2.0. It can be shown that RTS noise has a Lorentzian spectrum with a corner frequency  $f_c$  [7], which is the blinking frequency. It follows the following equation in the case of bi-stable RTS noise [13]:

$$S_{RTS}(f) = \frac{A^2}{f_c^2(\tau_1 + \tau_2)[1 + \left(\frac{f}{f_c}\right)^2]} \quad (2)$$

with  $A$  the RTS amplitude and  $\tau_{1,2}$  the respective mean lifetimes for each stable state. We can deduce that, in this case,  $\alpha_{RTS}=2.0$ . Thus it is represented in LFNS by an intense peak centered on  $f_c$ , while the  $1/f$  noise is flatlined by the  $f$ -normalization. The area of the peak is proportional to the square of the jump amplitude. This technique has the advantage of emphasizing the high-alpha sources of noise against the low-alpha ones. The main drawback is that this technique is not a self-sufficient detection technique, as we cannot distinguish RTS noise from Generation-Recombination (GR) noise. Both of them have Lorentzian spectra and therefore have the same signature in LFNS. In general, this method is used to study GR noise and carrier lifetime, another way of reducing low frequency noise in semiconductors. In our case, Low Frequency Noise Spectroscopy is a good technique to determine precisely an RTS pixel blinking frequency, and is robust to  $1/f$  low frequency noise, compared to temporal analysis.

Fig.3 presents a low frequency noise spectrum of a real pixel. It is fitted with a Lorentzian+white noise model and a value of blinking frequency is extracted. The PSD is estimated using the Welch periodogram method [14].

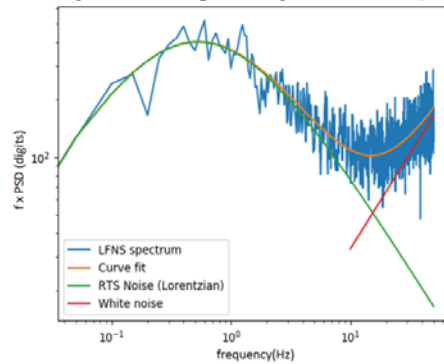


Fig. 3. Low Frequency Noise Spectrum of an 140K RTS pixel and the fitted model with its different contributions. The corresponding blinking frequency of the pixel is  $f_c=0.53$ Hz.

It is important to note that this blinking frequency is not representative of the whole infrared array. With a typical signal of 5k frames, the measurable blinking frequency ranges from 0.1Hz to 10Hz. Likewise, this Lorentzian+white noise model is only strictly suitable in the case of bi-stable RTS pixels, which have a Lorentzian PSD. The case of multi-stable RTS pixels is more complex. If the number of states is three, the system contains two related systems. They are either two independent systems with, coincidentally, the same amplitude, which brings us back to the aforementioned case, or two strongly correlated systems. The PSD of such a system is unclear and is not considered at the moment. This is the reason why only bi-stable pixels, which are predominant, will be considered in is paper.

### III. EXPERIMENTAL RESULTS

Experimental study has been realized on a 640x512 px<sup>2</sup>, 15μm pitch, blue Mid-Wave Infrared (MWIR) p-on-n HgCdTe R&D FPA from Sofradir [3]. Its cutoff frequency is  $\lambda_c = 4.2\mu\text{m}$  at 140K which is in the middle of the MWIR band. The FPA is integrated in a custom liquid nitrogen continuous flow cryostat which enables control of the sensor temperature. The sensor is polarized in reverse and placed in front of a blackbody with fixed temperature (typ. 25°C). A series of 7 measurements of 50K images with the detector temperature ranging from 120K to 155K has been performed, during the same thermal cycle. The framerate being 99.8 fps, the measurement timespan is approximately 501 s. For each measurement, each pixel with a sufficient noise is treated with the PELT algorithm. When a RTS pixel is detected, its parameters are calculated (jump amplitude, mean lifetime), the LFNS spectrum is computed and the LFNS blinking frequency is extracted. The proportion of RTS pixels detected for each measurement is shown in figure 4a). It is calculated by normalizing the number of RTS pixels by the highest one of the sequence (which is recorded at 155K). An exponential model is fitted with  $R^2=0.9988$ . Likewise, it is confirmed by the linear fit of the curve:  $\ln(N_{\text{RTS}}) = f(1000/T)$  with  $R^2=0.9977$  in fig. 2b).

We now have a confirmation that the number of RTS pixels inside a single MWIR blue FPA has a Boltzmann behavior. In parallel, it is also shown in figure 5 that blinking frequency is activated by temperature. Fig. 5b) shows superposed LFN spectra for the PELT-detected RTS pixel n°182113 whose temporal signal is shown in figure 5a). The temporal signal has been truncated to only 500 frames for visual convenience purposes, but the LFN spectra have been evaluated with the full signal, i.e. 50K images.

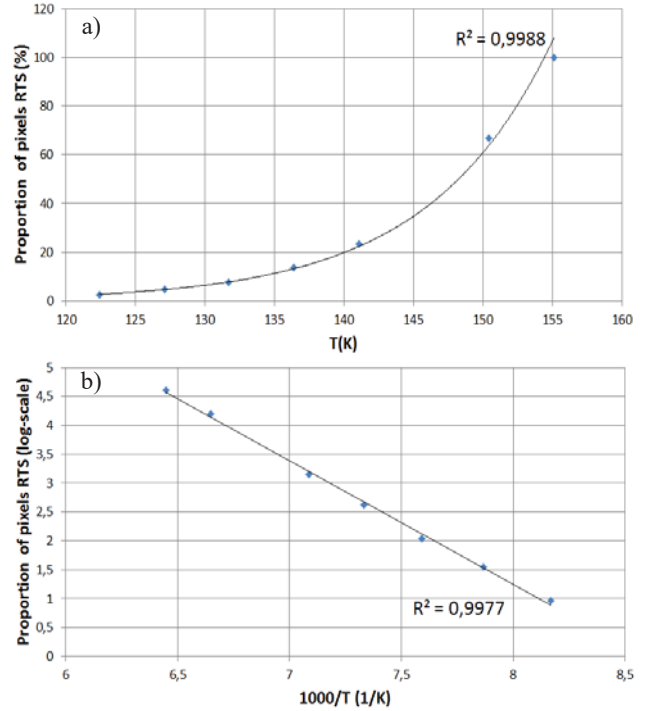


Fig. 4. a) Arrhenius curve  $N_{\text{RTS}}=f(T)$  of the number of RTS pixels and its exponential fitted model. b)  $\ln(N_{\text{RTS}})=f(1000/T)$  curve and its linear fitted model.

The blinking frequency and the area of the peak appear to increase with the temperature, as expected. Each spectrum is systematically fitted with our Lorentzian+white noise model. Fig.5c) shows the evolution of the normalized blinking frequency as a function of temperature for the same pixel. In the same way as the number of RTS pixels, it follows an Arrhenius law, which is coherent with the literature [3].

LFNS is a very straightforward and efficient way to obtain corner frequencies, but is limited by the experimental conditions. The highest obtainable frequency is linearly related to the ROIC. On the opposite, the lower measurable frequency is linear with the actual length of the experiment. However, in the case of standard 640x512 pixels FPAs, the amount of data resulting in very long experiments is huge and sometimes cannot be afforded. The minimum frequency is then a compromise between a windowing of the FPA and the amount of statistics on RTS pixels needed.

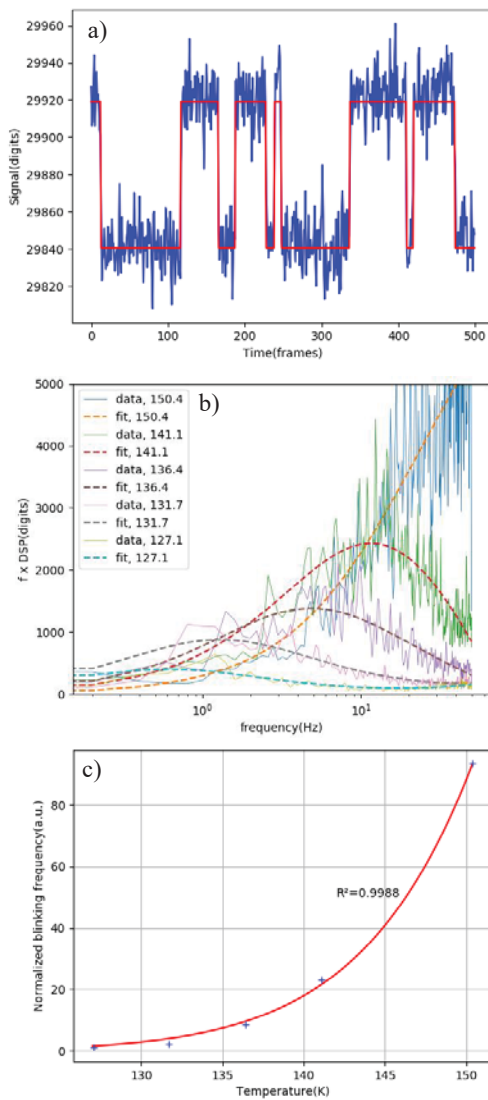


Fig. 5. a) Temporal signal of pixel n°182113 (in blue) and PELT fit (in red), truncated to 500 frames for viewing purpose. b) Low Frequency Noise Spectra of the same pixel with their fit for varying temperatures. c) Arrhenius curve of the blinking frequency of the same pixel. Blue dots are the measured value, red line is the fitted curve.

## CONCLUSION

In this paper, we used two complementary methods, one based on the analysis of the temporal signal using the PELT algorithm, and the other based on the analysis of the power spectral density using the LFNS method. The PELT changepoint method is a very efficient RTS detection method, and extracts amplitudes, lifetimes, and blinking frequency for bi-stable and multi-stable blinking pixels. To avoid false alarms, Low Frequency Noise Spectroscopy is applied in order to confirm the blinking frequency obtained with PELT (only for bi-stable pixels for now). A pixel that has gone through both algorithms with consistent values is

considered a true RTS. LFNS can also be used to study GR noise due to its similar spectral signature.

The validity of these methods has been demonstrated in the case of an Arrhenius law study. In parallel, this study confirmed the Boltzmann behavior of the number of RTS pixels and of the blinking frequency of an individual pixel. The next step in the study is to apply these methods to the whole RTS pool of pixels in the infrared FPA in order to estimate amplitude, mean lifetime and activation energy distributions. Those methods will be used to study the RTS phenomenon in cooled infrared FPA under different stress situations.

## REFERENCES

- [1] F. N. Hooge, "1/f noise sources," *IEEE Transactions on Electron Devices*, vol. 41, no. 11, pp. 1926-1935, Nov. 1994.
- [2] M. J. Uren, D. J. Day, and M. J. Kirton, "1/f and random telegraph noise in silicon metal-oxide-semiconductor field-effect transistors", *Applied Physics Letters* **47**, 1195 (1985).
- [3] L. Rubaldo *et al.* "State of the art HOT performances for Sofradir II-VI extrinsic technologies," Proc. SPIE 9819, *Infrared Technology and Applications XLII*, 98191I, 20 May 2016.
- [4] N. Pérè-Laperne *et al.*, "Latest developments of 10 $\mu$ m pitch HgCdTe diode array from the legacy to the extrinsic technology", *Infrared Technology and Applications XLII*. International Society for Optics and Photonics, 2016. p. 981920.
- [5] V. Arounassalame, J. Nghiem, M. Guénin, E. Costard, P. Christol, I. Ribet Mohamed, "Temporal stability measurements of a cooled infrared type II superlattice (T2SL) focal plane array detector", submitted to *2019 International Conference on Noise and Fluctuations (ICNF)*, Neuchatel.
- [6] I. Ribet-Mohamed, J. Nghiem, M. Caes, M. Guenin, L. Höglund, et al.. Temporal stability and correctability of a MWIR T2SL focal plane array. *QSIP 2018*, Jun 2018, Stockholm, Sweden. pp.145-150.
- [7] R. Killick, P. Fearnhead, and I. A. Eckley, "Optimal detection of changepoints with a linear computational cost", *J. Am. Stat. Assoc.*, Vol. 107, no 500, pp. 1590-1598, Dec. 2012.
- [8] A. Brunner, L. Rubaldo, V. Destefanis, F. Chabuel, A. Kerlain, D. Bauza, and N. Baier, "Improvement of RTS Noise in HgCdTe MWIR Detectors", *J. Electron. Mater.*, Vol. 43, no 8, pp 3060-3064, Aug 2014.
- [9] Y. Yuzhelevski, M. Yuzhelevski and G. Jung, "Random telegraph noise analysis in time domain", *Review of Scientific Instruments*, vol. 71, no 4, pp. 1681-1688, 2000.
- [10] B. K. Jones, "Low-frequency noise spectroscopy," in *IEEE Transactions on Electron Devices*, vol. 41, no. 11, pp. 2188-2197, Nov. 1994.
- [11] L. Ciura, A. Kolek, A. Kęłowski, D. Staszczek, A. Piotrowski, W. Gawron, and J. Piotrowski . "Investigation of trap levels in HgCdTe IR detectors through low frequency noise spectroscopy". *Semiconductor Science and Technology*, , vol. 31, no 3, p. 035004, 2016.
- [12] L. Ciura, A. Kolek, J. Wróbel and P. Martyniuk, "Low-frequency noise versus deep level transient spectroscopy of InAs/GaSb superlattice mid-wavelength infrared detectors," *2017 International Conference on Noise and Fluctuations (ICNF)*, Vilnius, , pp. 1-4, 2017.
- [13] S.Machlup, "Noise in Semiconductors: Spectrum of a Two-Parameter Random Signal", *Journal of Applied Physics* **25**, 341 (1954).
- [14] P. Welch, "The use of fast Fourier transform for the estimation of power spectra: a method based on time averaging over short, modified periodograms", *IEEE Transactions on audio and electroacoustics*, vol. 15, no 2, p. 70-73, 1967.